DOI: 10.1002/adsc.200600654

New C_2-Symmetric Diphosphite Ligands Derived from Carbohydrates: Effect of the Remote Stereocenters on Asymmetric Catalysis

M. Rosa Axet,[a] Jordi Benet-Buchholz,[b] Carmen Claver,[a,*] and Sergio Castillón[c,*]

[a] Departament de Química Física i Inorgànica, Universitat Rovira i Virgili, Marcelli Domingo s/n, 43007 Tarragona, Spain
Fax: (+34)-97-755-9563; e-mail: carmen.claver@urv.cat
[b] Institute of Chemical Research of Catalonia (ICIQ), Av. Països Catalans 16, 43007 Tarragona, Spain
[c] Departament de Química Analítica i Química Orgànica, Facultat de Química, Universitat Rovira i Virgili, Marcelli Domingo s/n, 43007 Tarragona, Spain; e-mail: sergio.castillon@urv.cat

Received: December 31, 2006

Supporting information for this article is available on the WWW under http://asc.wiley-vch.de/home/.

Abstract: The synthesis of new modular chiral diphosphite ligands with C_2-symmetry and carbohydrate backbone is reported. We also report here the synthesis of the corresponding rhodium complexes $[Rh(COD)(L)]BF_4$ (L = diphosphite). All these species have been characterised in solution by NMR spectroscopy and in some cases in the solid state by X-ray diffraction. The solution structures of the hydridorhodiumcarbonyl species $[RhH(CO)_2(L)]$, where L = diphosphites **12a**–**14a**, **12b**, have been studied using high-pressure NMR spectroscopy. The configuration and substitution of the remote stereocentres in positions 2 and 5 of the tetrahydrofuran ring of the diphosphite ligands were observed to have a considerable influence on the results obtained in the rhodium-catalysed hydroformylation and hydrogenation reactions. Thus, the configuration of the major isomer obtained in the hydroformylation reaction may be controlled by changing the configuration of these stereocentres.

Keywords: asymmetric catalysis; carbohydrates; diphosphites; hydroformylation; hydrogenation

Introduction

In homogeneous asymmetric catalysis based on transition metals, the design of new ligands is, perhaps, the most crucial step to achieve the highest levels of reactivity and selectivity. One of the simplest ways of obtaining chiral ligands is to transform natural chiral compounds, thus making optical resolution procedures unnecessary. This fact, that can be considered an advantage from a synthetic point of view, is also one limitation for catalytic purposes, since only one enantiomer is accessible. However, this limitation may be partially overcome by using the so-called pseudoenantiomer ligands as will be shown in this contribution. Carbohydrate derivative ligands have many advantages: they are readily available, highly functionalised, and they may be systematically modified.[1] Some carbohydrate derivative ligands are showed in Figure 1. The pyranoside diphosphinite ligands **1** were successfully used in rhodium-catalysed asymmetric hydrogenation of enamido acids,[2] and nickel-catalysed hydrocyanation of alkenes.[3] Ligand **2** proved to function as a pseudoenantiomer of **1** providing the opposite enantiomer in the asymmetric hydrogenation of prochiral olefins.[4]

During the last years we have focused in the use of furanose derivatives of C_1-symmetry as ligands in asymmetric catalysis. Some of these ligands have been

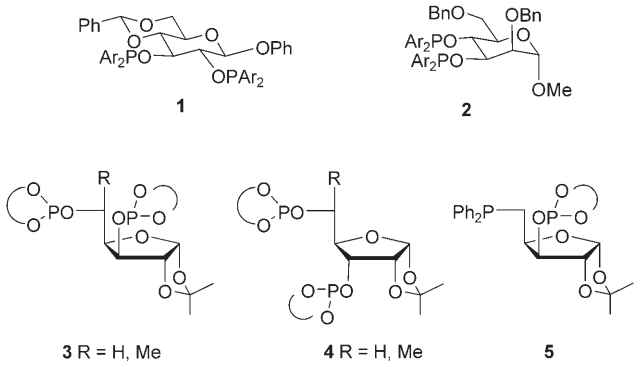

Figure 1. Representative carbohydrate derivative ligands (**1**–**5**) with pyranoid and furanoid skeleton.

successfully applied in metal-catalysed asymmetric reactions providing excellent results in rhodium-catalysed asymmetric hydrogenation, asymmetric hydroformylation or palladium-catalysed asymmetric allylic substitution.[1] Particularly interesting are the catalytic results obtained in the rhodium-catalysed asymmetric hydroformylation of vinylarenes with C_1-symmetric diphosphites derived from carbohydrates, **3** (R = methyl) (Figure 1),[5,6] which are some of the best reported so far.[7,8] Both the *S* and the *R* enantiomers can be obtained with excellent regio- and enantioselectivity (91%, 98%) under mild reaction conditions. The configuration of the stereocenters (C-3, C-5) had remarkable effects on the enantioselectivity of the hydroformylation reactions as was shown through the characterisation of the solution structures of the hydridorhodium diphosphite dicarbonyl intermediates $[RhH(CO)_2(L)]$.[5,6] Complexes containing ligands **4** and **5** were used in the asymmetric hydrogenation of prochiral olefins also leading to excellent results[9–11] Recently, palladium nanoparticles stabilized by ligand **3** (R = H) were used in the allylic alkylation reaction providing an excellent kinetic resolution.[12]

Ligands with C_2-symmetry are in general prepared from D-mannitol. Reetz et al.[13] reported the use of diphosphites **6** in the asymmetric hydrogenation of acetoamidoacrylic acid derivatives achieving enantioselectivities up to 98%. Other remarkable C_2-symmetric ligands, derived from mannitol, successfully applied in asymmetric hydrogenation are the 2,5-disubstitued phospholane ligands (Duphos derivatives) **7** and **8**[14] and the related DIOP,[15] analogue. These 2,5-disubstitued phospholane ligands have recently been identified as excellent ligands for the rhodium-catalysed asymmetric hydroformylation providing high turnover rates and enantioselectivities for styrene, allyl cyanide, vinyl acetate[16] and [2.2.1]-bicyclic olefins.[17]

We have recently reported the synthesis of C_2-symmetric diphosphinite ligands **9** and **10** derived from carbohydrates with a furanoid backbone.[18] These ligands were used in the rhodium-catalysed asymmetric hydrogenation of olefins. The use of ligands **9** and **10** (Figure 2) in the hydrogenation of enamido esters considerably improves the enantioselectivity in comparison with the results obtained with ligand **11**,[19] which does not have substituents in the remote stereocentres. Since the configuration of carbon bonded to the phosphinite function is similar in all these ligands, this result reveals a remarkable influence of the substituents in positions 2 and 5 of the tetrahydrofuran ring.

In order to know more about this remote effect in asymmetric catalysis, we present here the preparation of a new family of diphosphite ligands **12–14** (Figure 3). These ligands present important differences in respect to the previous C_1-symmetric phosphite ligands because, instead the rigid bicycle of the xylose and glucose derivatives, they contain substituents in positions 2 and 5 of the sugar backbone. This fact allows us to study the influence on the enantioselectivity of different substituents present at C-2 and C-5, and the configuration of these positions. We also report here the synthesis of the corresponding rhodium cationic complexes containing the chiral ligands **12–14** and their application in the rhodium-catalysed asymmetric hydroformylation of vinylarenes and hydrogenation of methyl acetamidoacrylate.

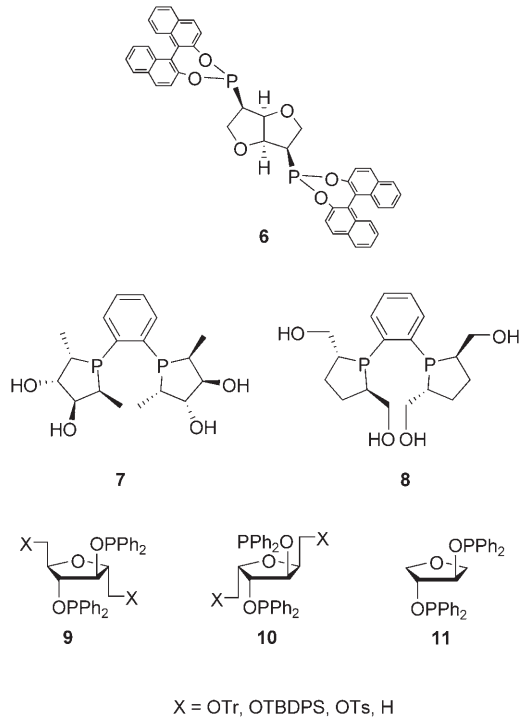

Figure 2. C_2-Symmetric ligands **6–11**. Ligands **6–10** were obtained from carbohydrates.

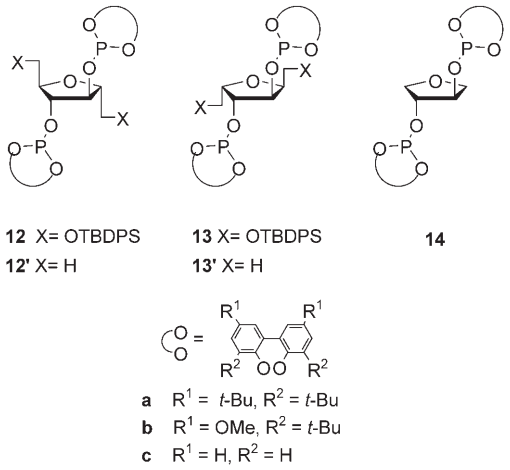

Figure 3. New C_2-symmetric diphosphite ligands **12–14**.

Results and Discussion

Synthesis of Diphosphite Ligands with Carbohydrate Backbone

Diphosphite ligands **12–13** were synthesised from the diols **17** and **21**, respectively, which in turn were prepared in a straightforward manner from D-glucosamine and D-glucitol, respectively (Scheme 1 and Scheme 2).

Thus, tetrol **16** was prepared from D-glucosamine following reported procedures.[18] To study the steric effect of the groups in positions 2 and 5 we selected a silyloxymethyl and a methyl groups. The reaction of **16** with *tert*-butyldiphenylchlorosilane (TBDPSCl) afforded the diol **17** in high yield, resulting from the selective protection of the primary alcohols. To obtain the diol **17′** with a methyl group at positions 2 and 5, the primary hydroxy groups of **16** were selectively ditosylated[20] and then treated with $LiAlH_4$ to afford compound **17'** (Scheme 1).[18,20] Diols **17** and **17′** were treated with phosphorochloridites **18a–c**, synthesised *in situ* by standard procedures,[21,22] to give the corresponding diphosphites **12a–c** and **12′a**, **b** in moderate to good yields (31–72%).

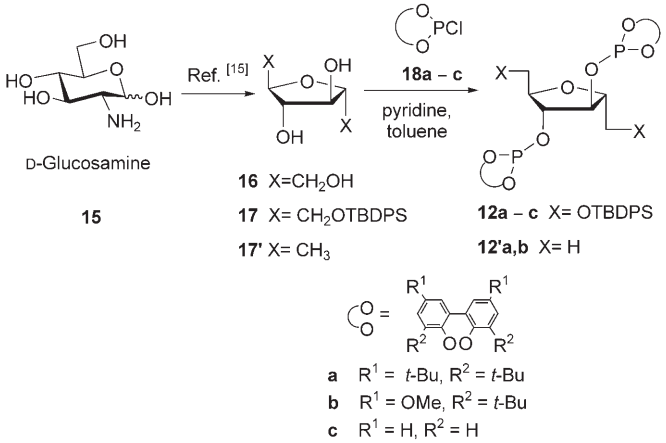

Scheme 1. Synthesis of 2,5-anhydro-D-mannitol derivative ligands **12a–c** and **12′a**, **b**.

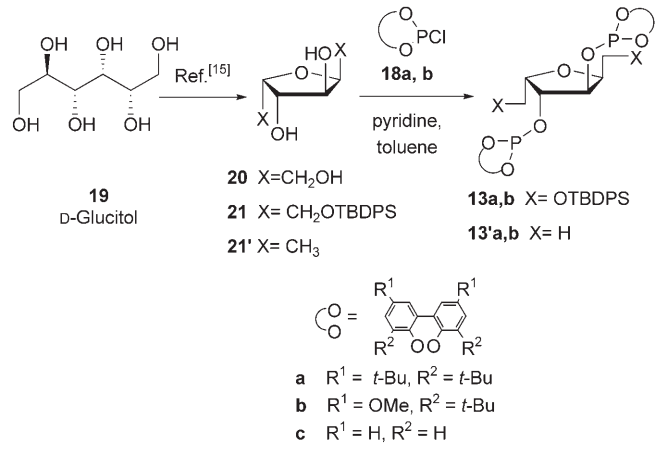

Scheme 2. Synthesis of 2,5-anhydro-L-iditol derivative ligands **13a**, **b** and **13′a**, **b**.

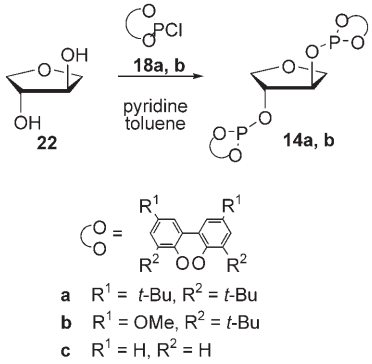

Scheme 3. Synthesis of (3*R*,4*R*)-3,4-dihydroxytetrahydrofuran derivative ligands **14a**, **b**.

Tetrol **20** was obtained from D-glucitol (**19**) following a reported procedure.[23] Primary alcohols were also protected by reaction with TBDPSCl to give compound **21**. The 2,5-dimethyl derivative **21′** was obtained by selective ditosylation of **20** and further reduction with $LiAlH_4$ (Scheme 2).[18,20] Treatment of **21** and **21′** with phosphorochloridites **18a**, **b**[21,22] gave the corresponding diphosphites **13a**, **b** and **13′a**, **b** in moderate to good yields (32–92%).

The diphosphite ligands **14a**, **b**, which do not contain substituents in positions 2 and 5 were also prepared by reaction of (3*R*,4*R*)-3,4-dihydroxytetrahydrofuran **22**[24] with phosphorochloridites **18a**, **b**[21,22] in 75 and 25% yield, respectively (Scheme 3).

The structures of diphosphite ligands **12–14** were determined by one-dimensional ^{1}H,$^{13}C\{^{1}H\}$ and $^{31}P\{^{1}H\}$ NMR. The signals were readily assigned by using bidimensional COSY and HSQC techniques. The $^{31}P\{^{1}H\}$ NMR spectrum of ligands **12–14** showed a single signal, located between 140 and 147 ppm, characteristic of a phosphite function. However, between 3–5 ppm of the ^{1}H NMR spectra of ligands **12–14** appeared signals characteristic of second-order spectra, as a consequence of the existence of $AA'BB'X_2X'_2$ (**12–13**) or $AA'BB'X_3X'_3$ (**12′–13′**) spin systems.

The crystal structure of diphosphite ligand **12a** was determined by X-ray diffraction. Monocrystals of **12a** suitable for X-ray diffraction were obtained by slow diffusion of hexane into a CH_2Cl_2 solution of the ligand. The ligand crystallises as a solvate containing two molecules of *n*-hexane in the elementary cell. The central five-membered ring has a twisted conformation (Figure 4 and Figure 5). This ligand was found to crystallise as a racemic twin (74:16).

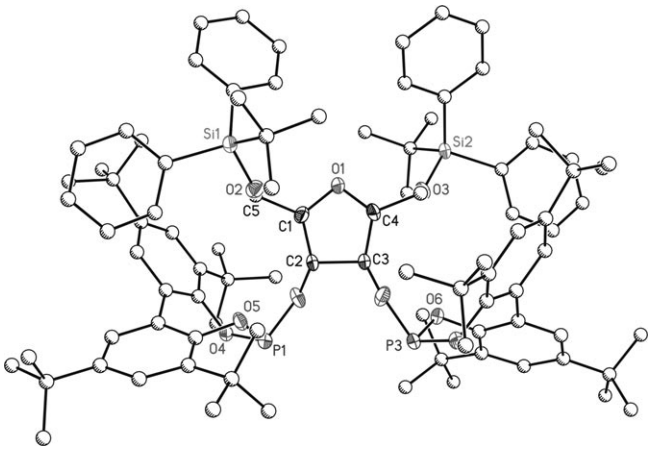

Figure 4. Structure model (ellipsoids at 50% probability level) of ligand **12a**. Counterions, solvates and hydrogen atoms have been omitted for the sake of clarity.

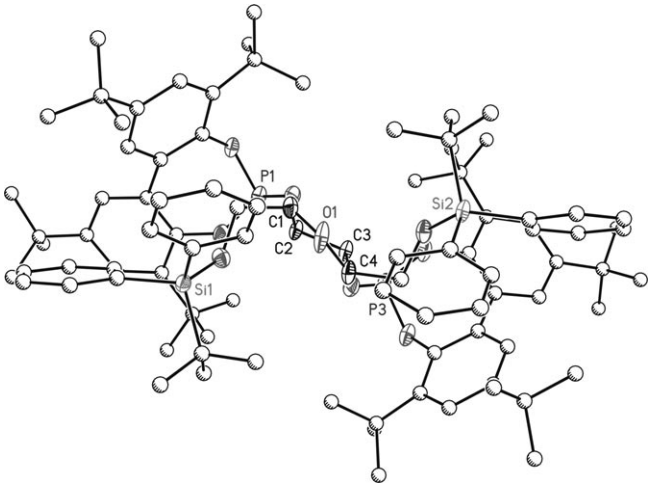

Figure 5. Structure model showing a lateral view of the ligand **12a**.

Synthesis of the Rhodium Complexes

Rhodium complexes $[Rh(COD)(L)]BF_4$, **23**–**25**, where L = diphosphite ligands **12**–**14** and COD = cyclooctadiene, were prepared by reacting $[Rh(COD)_2]BF_4$ with ligands **12a**–**c**, **12′a**, **b**, **13a**, **13′a** and **14a**, **b**, respectively (Scheme 4). All complexes were isolated as air-stable coloured solids. The structure of the rhodium complexes **23**–**25** was elucidated by NMR spectroscopy techniques. The NMR spectra of the complexes at 25 °C show that they retain the C_2-symmetry in solution. In the $^{31}P\{^1H\}$ NMR spectrum, only one signal appeared between 127 and 136 ppm ($J_{P\text{-}Rh}$ = 253–256 Hz). The chemical shift and coupling constant values are in agreement with those observed for related cationic diphosphite rhodium complexes.[10,11] The ^1H and ^{13}C NMR chemical shifts were similar to those of the free ligands, and the 1,5-cyclooctadiene ligand showed two groups of signals between 4.65 and 5.88 ppm, and between 1.94 and 2.34 ppm for the methynic and methylenic groups, respectively. The mononuclearity of the complexes was confirmed by MALDI spectra, which in all cases showed molecular ions corresponding to the cation $[Rh(COD)(L)]^+$ (L = **12a**–**c**, **12′a**–**b**, **13a**, **13′a** and **14a**, **b**).

Monocrystals of the complexes [Rh(COD)(**12a**)]BF_4 (**23a**) and [Rh(COD)(**13′a**)]BF_4 (**24′a**) were obtained by slow diffusion of hexane into a CH_2Cl_2 solution of the complex. Compound [Rh(COD)(**12a**)]BF_4 (**23a**) crystallises as a cation together with a BF_4^- anion (Figure 6 and Figure 7). The rhodium atom is coordinated in a slightly distorted square planar geometry with a mean deviation from the plane of 0.101 Å. The distances between the metal atom and the centres of the double bonds at the cyclooctadiene rings are: 2.17 Å and 2.18 Å. The five-membered ring has a twisted conformation. This compound crystallises as a single enantiomer in a pure chiral structure. Compound [Rh(COD)(**13′a**)]BF_4 (**24′a**) crystallises with two independent cations in the elementary cell (Figure 8, Figure 9, Figure 10 and

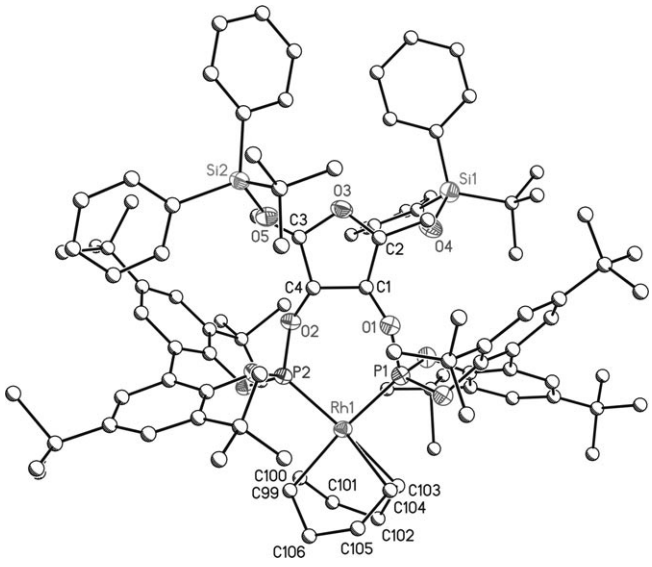

Figure 6. Structure model (ellipsoids at 50% probability level) of [Rh(COD)(**12a**)]BF_4 (**23a**). Counterions, solvates and hydrogen atoms have been omitted for the sake of clarity.

$$[Rh(COD)_2]BF_4 + \text{diphosphite} \longrightarrow [Rh(COD)(\text{diphosphite})]BF_4 + COD$$

12 – 14 **23 – 25**

Scheme 4. Synthesis of cationic rhodium complexes **23**–**25**.

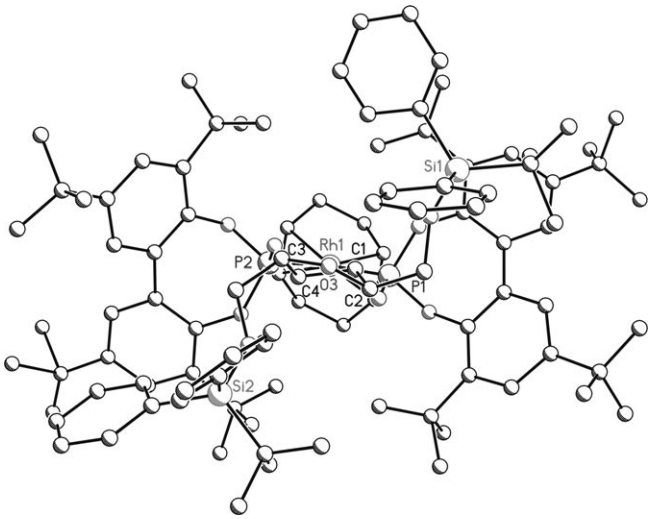

Figure 7. Lateral view of the complex [Rh(COD)(**12a**)]BF_4 (**23a**).

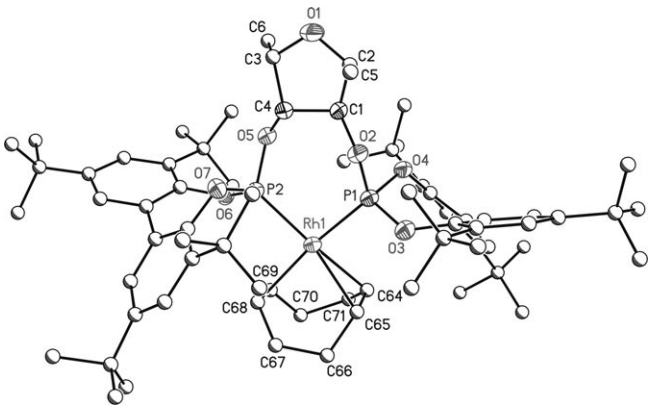

Figure 8. ORTEP diagram of [Rh(COD)(**13′a**)]BF_4 (**24′a**), molecule A. Counterions, solvates and hydrogen atoms have been omitted for the sake of clarity.

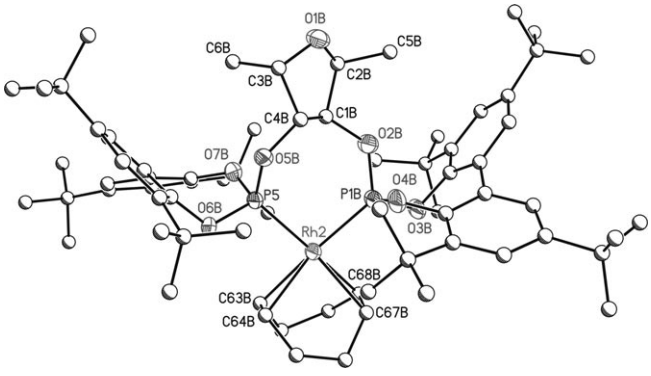

Figure 9. ORTEP diagram (ellipsoids at 50% probability level) of [Rh(COD)(**13′a**)]BF_4 (**24′a**), molecule B. Counterions, solvates and hydrogen atoms have been omitted for the sake of clarity.

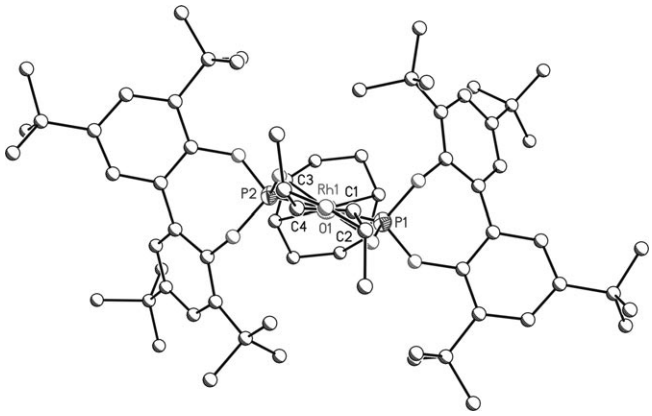

Figure 10. Lateral view of [Rh(COD)(**13′a**)]BF_4 (**24′a**), molecule A.

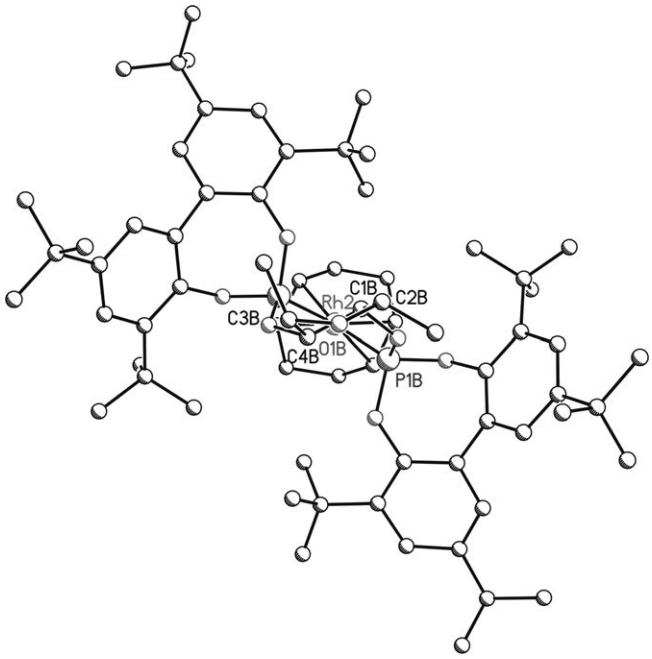

Figure 11. Lateral view of [Rh(COD)(**13′a**)]BF_4 (**24′a**), molecule B.

Figure 11). The independent cations detected in the crystal cell differ in their conformation. In molecule A, the five-membered ring has a twisted conformation and in molecule B this ring has an envelope conformation. The seven-membered ring formed by the metal atom also shows different folding in molecules A and B. For molecule B, the folding of this seven-membered ring is more pronounced. In both molecules the rhodium atom is coordinated in a slightly distorted square planar geometry. In molecule A, the mean deviation from the plane is 0.041 Å and in molecule B the mean deviation from plane is 0.081 Å. The distances between the metal atom and the centres of the double bonds at the cyclooctadiene rings are in molecule A: 2.22 Å and 2.20 Å and in molecule B:

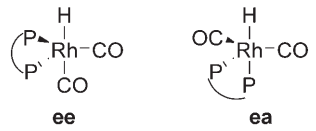

Figure 12. Equatorial-equatorial (**ee**) and equatorial-axial (**ea**) $[RhH(CO)_2(L)]$ species.

2.25 Å and 2.26 Å. This complex crystallises in a pure chiral structure.

The distances and angles measured for this species are similar to those previously described for the rhodium-diphosphinite complex **9** (X = H) (Figure 2), where the diphosphinite ligand has the same furanoside backbone.[18]

High-Pressure NMR Study

The hydridorhodium diphosphite complexes $[RhH(CO)_2(L)]$ (L = bidentate ligand) are generally considered to be the resting state in the hydroformylation reaction.[8,25–27] It is generally assumed that they have a trigonal-bipyramidal structure. Two isomeric structures of these complexes can be formed with a coordinated bidentate ligand (Figure 12). The presence of only one active diastereoisomeric hydridorhodiumcarbonyl species with bidentate ligands is presumably the key to an efficient control of the chirality transfer.[28] These two isomeric structures can be easily distinguished by NMR, since the complexes with **ee** (equatorial-equatorial) coordination show $J_{P\text{-}H} < 10$ Hz, and $J_{P\text{-}P} = 250$ Hz whereas for *trans* coordinated phosphite, **ea** (equatorial-axial) complex $J_{P\text{-}H} = 180$–200 Hz and $J_{P\text{-}P} = 70$ Hz.[28–31] To obtain information about these species, we studied the solution structures of the hydridorhodium diphosphite dicarbonyl species $[RhH(CO)_2(L)]$, where L = diphosphites **12a**–**14a**, **12b**, through high-pressure NMR spectroscopy. Under typical hydroformylation conditions, [Rh(acac)(L)] (acac = acetylacetonate) complexes transform to trigonal bipyramidal hydridorhodium diphosphites (Scheme 5).[28]

The complexes were prepared by adding one equivalent of diphosphite ligands **12a–14a**, **12b** to a toluene-d_8 solution containing $[Rh(acac)(CO)_2]$. In all cases a fast change of colour and displacement of CO were observed. The initial solution was analysed by ^{31}P and ^{1}H NMR spectroscopy. Later the NMR tube was pressurised with syngas (20 bar) and heated at 80 °C for 30 min and the ^{31}P and ^{1}H NMR spectra were then recorded. Finally the NMR tube was shaken for 15 h at 80 °C and NMR spectra were again recorded.

Initially, the displacement of two carbon monoxide molecules by the diphosphite ligands yields the [Rh(acac)(L)] complexes which, after a short time under hydroformylation conditions, evolved to the species [Rh(acac)(CO)(L)] with characteristic rhodium-phosphorus coupling constants (*ca.* 300 Hz) (Scheme 5).[30,31] We observed these species in all cases except for ligands **12a** and **12b**, which directly formed the hydridorhodiumdicarbonyl complexes $[RhH(CO)_2(L)]$ from [Rh(acac)(L)]. After a reaction time of 15 h the solution was analysed at room temperature and, in all cases, stable $[RhH(CO)_2(L)]$ complexes were exclusively obtained. This was confirmed by the presence in the $^{31}P\{^{1}H\}$ NMR spectrum of a doublet around 155 ppm ($J_{P\text{-}Rh} = 230$ Hz) and in the ^{1}H NMR spectrum of a signal at −10 ppm. Small amounts of the phosphonate, signal at 10 ppm in the $^{31}P\{^{1}H\}$ NMR spectrum, were also detected.

Structural Assignments

The $^{31}P\{^{1}H\}$ NMR chemical shifts (in ppm) and the coupling constants (in Hertz) of $[RhH(CO)_2(L)]$ (L = **12a–14a**, **12b**) complexes are summarised in Table 1. These complexes showed somewhat broadened doublets at room temperature in the $^{31}P\{^{1}H\}$ NMR spectra. These broad signals suggest a fluxional process on the NMR time scale.[25] The doublets appeared between 152.7 and 158.1 ppm with $^{1}J_{Rh\text{-}P}$ coupling constants between 230.0 and 234.1 Hz. These large $^{1}J_{Rh\text{-}P}$ coupling constants indicate that the ligands coordinate in an equatorial-equatorial fashion in the trigonal-bipyramidal hydridorhodiumcarbonyl species.[28–31] In the ^{1}H NMR spectrum the hydride signal was detected at $\delta = -10$ ppm. The $^{1}J_{Rh\text{-}H}$ coupling constants were in the range of 2.0 to 3.8 Hz and the $^{2}J_{P\text{-}H}$ coupling constants were between 2.0 and 9.0 Hz. These small phosphorus-hydrogen coupling constants (< 10 Hz) explain that the hydride signal appears as a

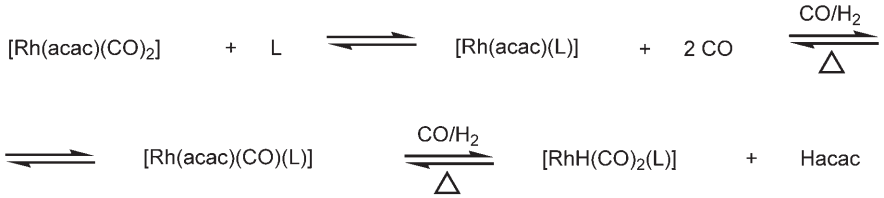

Scheme 5. Formation of $[RhH(CO)_2(L)]$ from $[Rh(acac)(CO)_2]$ and diphosphites **12a–14a, 12b** (L).

Table 1. Selected ^1H and $^{31}P\{^1H\}$ NMR data for $[RhH(CO)_2(L)]$ complexes.[a]

Ligand	δ (^{31}P)[b]	δ (^1H)[b]	$^1J_{Rh\text{-}P}$[c]	$^1J_{Rh\text{-}H}$[c]	$^2J_{P\text{-}H}$[c]
12a	152.70 (d)	−9.93 (br t)	231.9	2.0	2.0
12b	155.33 (d)	−9.91 (q)	230.0	3.4	3.9
12′a	155.43 (d)	−10.14 (q)	231.6	2.7	3.8
13a	158.09 (d)	−9.85 (q)	233.6	2.9	3.1
13′a	155.27 (d)	−10.05 (q)	234.1	3.8	3.9
14a	156.40 (d)	−10.24 (dt)	232.6	3.4	9.0

[a] Prepared in toluene-d_8 by adding 1.1 equivalents of ligand to the $[Rh(acac)(CO)_2]$ solution, 15 h. at 80 °C under 20 bars of syn gas.
[b] ^{31}P and ^1H NMR spectra recorded in toluene-d_8 using a 10-mm high-pressure NMR tube. Chemicals shifts δ in ppm (multiplicity).
[c] Coupling constants in Hz.

quadruplet in most of the cases, except for the complex containing ligands **12a** and **14a**. In the case of ligand **14a** a doublet of triplets was observed in the hydride region and indicates a *cis* configuration between the phosphorus atoms and the hydride ligand.

Low Temperature Studies

As a consequence of the C_2-symmetry of the ligands, the phosphorus atoms are equivalent in the free ligand. However, this is not the case for the hydridorhodiumcarbonyl diphosphite complexes $[RhH(CO)_2(L)]$ (L = **12–14**), where, although both phosphorus atoms are coordinated in an equatorial-equatorial fashion to the rhodium centre, the complex has a C_1-symmetry. The fact that only one doublet is observed in the $^{31}P\{^1H\}$ NMR spectrum indicates that either the chemical shifts of both atoms accidentally coincide or that they exchange rapidly on the NMR time scale.[28–31] An NMR study of the hydridorhodiumcarbonyl species was performed at low temperature in the presence of CO and H_2. Selected ^1H and $^{31}P\{^1H\}$ NMR data for $[RhH(CO)_2(L)]$ complexes at low temperature are summarised in Table 2.

The behaviour of these species strongly depends on the structure of the diphosphite ligands. Complexes $[RhH(CO)_2(L)]$ where L = **12a**, **12b** and **12′a**, derived from 2,5-anhydro-D-mannitol, all showed similar behaviour. When the temperature was decreased, broadening of the resonance of the $^{31}P\{^1H\}$ NMR and in the hydride region of the ^1H NMR spectra was observed. The signals of the $^{31}P\{^1H\}$ NMR for complexes $[RhH(CO)_2(L)]$, where L = **12a** and **12′a**, were resolved at −100 °C (Figure 13). Two doublets of doublets in the $^{31}P\{^1H\}$ NMR spectrum were detected: one signal at *ca.* δ = 160, and the other at δ = 150. The coupling constants, $^1J_{Rh\text{-}P1}$ around 270 Hz and $^1J_{Rh\text{-}P2}$ around 230 Hz, and $^2J_{P\text{-}P}$ around 300 Hz, indicated that the ligand was coordinated in an equatorial-equatorial fashion. The hydride region of the ^1H NMR

Table 2. Selected ^1H and $^{31}P\{^1H\}$ NMR data for $[RhH(CO)_2(L)]$ (L = **12a–14a, 12b**) complexes at low temperature.[a]

Ligand	δ (^{31}P)[b]		$^1J_{Rh\text{-}P1}$[c]	$^1J_{Rh\text{-}P2}$[c]	$^2J_{P\text{-}P}$[c]	T [°C]
12a	161.56 (dd)	148.21 (dd)	270.9	230.2	302.2	−100
12b	153.92 (broad)		Unresolved			−80
12′a	164.42 (dd)	153.62 (dd)	269.3	232.6	305.1	−100
13a	160.30 (dd)	156.75 (dd)	230.1	240.4	314.2	−80
13′a	157.49 (broad d)		238.6		-	−100
14a	158.68 (broad d)		233.5		-	−80

[a] Prepared in toluene-d_8 by adding 1.1 equivalents of ligand to the $[Rh(acac)(CO)_2]$ solution, 15 h. at 80 °C under 20 bars of syn gas.
[b] ^{31}P and ^1H NMR spectra recorded in toluene-d_8 using a 10-mm high-pressure NMR tube. Chemicals shifts δ in ppm (multiplicity).
[c] Coupling constants in Hz.

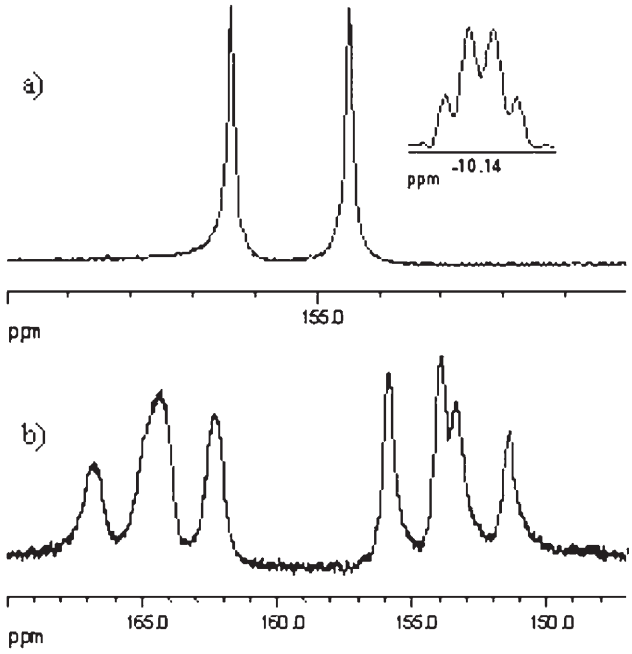

Figure 13. Selected regions of the ^1H and $^{31}P\{^1H\}$ NMR spectra of the complex $[RhH(CO)_2(\mathbf{12'a})]$ formed from the precursor $[Rh(acac)(CO)_2]$ in the presence of ligand **12′a** under hydroformylation conditions (15 h at 80 °C and 20 bar of syn gas) in toluene-d_8. a) Spectrum recorded at room temperature and b) spectrum recorded at −100 °C.

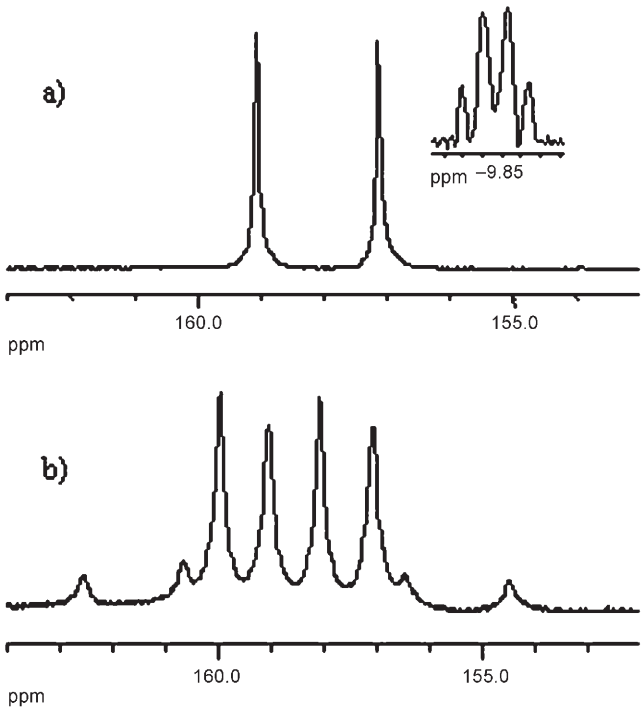

Figure 14. Selected regions of the ^{1}H and $^{31}P\{^{1}H\}$ NMR spectra of the complex $[RhH(CO)_2$(**13a**)] formed. from the precursor $[Rh(acac)(CO)_2]$ in the presence of ligand **13a** under hydroformylation conditions (15 h at 80 °C and 20 bar of syn gas) in toluene-d_8. a) Spectrum recorded at room temperature and b) spectrum recorded at −80 °C.

spectrum was not resolved and exhibited a broad signal at this temperature.

For the $[RhH(CO)_2$(**13a**)] complex, where diphosphite ligand **13a** is derived from 2,5-anhydro-L-iditol, the decrease in the temperature also led to broadening of the signals in the $^{31}P\{^{1}H\}$ and in the hydride region of the ^{1}H NMR spectra. The $^{31}P\{^{1}H\}$ NMR was better resolved at −80 °C, an eight-line spectrum for phosphorus atoms was observed. This arises from an ABX system where $^{1}J_{Rh\text{-}P1}$ and $^{1}J_{Rh\text{-}P2}$ are very close, 230 and 240 Hz, and the signals appeared at 160.30 and 156.75 ppm with a phosphorus-phosphorus coupling constant of 314.2 Hz (Figure 14). These coupling constants indicated an equatorial-equatorial coordination mode.

In the variable temperature study of the hydridorhodiumdicarbonyl complexes with ligands **13′a** and **14a** only a slight broadening of the doublet in the corresponding $^{31}P\{^{1}H\}$ at −80 °C was observed. This indicates that the fluxional process at this temperature is not completely stopped, suggesting a lower energy barrier than in the case of ligands **12a**, **12b**, **12′a** and **13a**.

The equatorial-axial coordination mode in the trigonal bipyramidal hydridorhodium-dicarbonyl species was previously reported with ligands that form seven-membered rings with the metal.[28,30,31] These new carbohydrate derivative ligands **12–14** were therefore expected to show similar coordination. However, this was not observed for ligands **12–14**, which coordinate in an equatorial-equatorial fashion (corroborated by the large $^{1}J_{Rh\text{-}P}$ and $^{2}J_{P\text{-}P}$ coupling constants and small $^{2}J_{P\text{-}H}$ coupling constants, observed in the NMR spectra). This coordination may be due to the rigidity of the ligands due to the presence of the tetrahydrofuran backbone.

Hydroformylation of Vinylarenes

The chiral diphosphites **12–14** were used as ligands in the rhodium-catalysed asymmetric hydroformylation of styrene and related prochiral olefin. The catalyst was prepared *in situ*. The diphosphite ligand was added to a solution of $[Rh(acac)(CO)_2]$ (acac = acetylacetonate) in toluene followed by the addition of the substrate. Afterwards the solution was introduced in an autoclave and pressurised with CO/H_2. The results of the asymmetric hydroformylation of styrene are given in Table 3 and Table 4. Neither hydrogenated nor polymerised products were observed.

The conditions were optimised with ligands **12a–c** (Table 3). An Rh/L ratio of 1/2 was found to be appropriate in order to increase the enantioselectivity in comparison to an Rh/L ratio of 1/1, although the activity decreases under these conditions. (Table 3, entries 3 *vs.* 4 and 9 *vs.* 11). This may be explained by the formation of the species $[RhH(CO)_4]$ at low Rh/L

Table 3. Rhodium-catalysed hydroformylation of styrene using diphosphites **12a** and **12b**.[a]

Entry	L	Rh/L	*t* [h]	*T* [°C]	% conversion[b]	% regioselectivity[c]	% *ee*
1	**12a**	1/1	15	60	99	78	20 (*S*)
2	**12a**	1/2	15	40	57	96	41 (*S*)
3	**12a**	1/1	48	25	>99	93	20 (*S*)
4	**12a**	1/2	48	25	77	97	46 (*S*)
5	**12a**[d]	1/2	48	25	85	97	42 (*S*)
6	**12b**	1/1	15	60	99	79	24 (*S*)
7	**12b**	1/1	15	40	99	88	28 (*S*)
8	**12b**	1/2	15	40	64	93	30 (*S*)
9	**12b**	1/1	48	25	>99	95	30 (*S*)
10	**12b**[d]	1/1	48	25	99	94	25 (*S*)
11	**12b**	1/2	48	25	97	93	39 (*S*)
12	**12b**	1/4	48	25	61	95	37 (*S*)
13	**12c**	1/1	15	60	99	79	0

[a] Substrate/Rh = 200, styrene 2.7 mmol, $[Rh(acac)(CO)_2]$ 0.0135 mmol, P = 20 bar, 15 mL toluene $P(CO/H_2) = 1$.
[b] % conversion of styrene determined by GC.
[c] % of 2-phenylpropanal
[d] $P(CO) = 10$, $P(H_2) = 20$.

Table 4. Rhodium-catalysed hydroformylation of styrene using diphosphites **12–14**.[a]

Entry	L	% conversion[b]	% regioselectivity[c]	% *ee*
1	**12a**	57	96	41 (*S*)
2	**12b**	64	93	30 (*S*)
3	**12′a**	98	93	14 (*R*)
4	**12′b**	98	94	19 (*R*)
5	**13a**	57	95	22 (*R*)
6	**13b**	40	98	43 (*R*)
7	**13′a**	33	96	17 (*S*)
8	**13′b**	25	94	18 (*S*)
9	**14a**	43	>99	26 (*R*)
10	**14b**	38	94	34 (*R*)

[a] Substrate/Rh = 200, Rh/L = 0.5, styrene 2.7 mmol, [Rh(acac)(CO)$_2$] 0.0135 mmol, P = 20 bar, 15 mL toluene, P-(CO/H$_2$) = 1, T = 40 °C, reaction time: 15 h

[b] % conversion of styrene determined by GC.

[c] % of 2-phenylpropanal.

ratios, which is known to be a highly active achiral hydroformylation catalyst.[28] However, a further increase of the Rh/L ratio (1/4) was not found to enhance the regioselectivity or the enantioselectivity (Table 3, entries 11 *vs.* 12), indicating that only a low excess of free ligand is needed in order to avoid the formation of [RhH(CO)$_4$] species. Concerning the effect of the partial pressure of hydrogen, we observed no improvement in the activity, the regioselectivity or the enantioselectivity when the H$_2$/CO ratio was changed to 2 at total pressure of 30 bar (Table 3, entries 4 *vs.* 5 and 9 *vs.* 10). In previous studies using rhodium systems containing diphosphite ligands with C_1-symmetry have shown a different behaviour, increasing the activity with the partial pressure of hydrogen.[6] The fact that the activity did not increase when the partial pressure of hydrogen was increased suggests that the rate-determining step is not the hydrogenolysis. As was expected, lower temperatures led to a decrease in the activity, thus the reaction time was increased to 48 h at 25 °C in order to have comparable conversions to those obtained at 40 °C for 15 h (e.g., Table 3, entries 7 *vs.* 10). A slight increase in the enantioselectivities (Table 3, entries 2 *vs.* 4 and 8 *vs.* 11) was also observed when the temperature was decreased.

For comparative purposes, ligands **13–14** were tested under conditions that gave the optimum compromise between enantioselectivities and reaction rates; i.e., Rh/L = 1/2, PCO/H$_2$ = 20 bar (1/1) and T = 40 °C. The results are given in Table 4.

A comparison of the conversions obtained with different catalysts that incorporate ligands derived from mannitol **12**, iditol **13** and dihydroxytetrahydrofuran **14**, showed that the systems containing ligands **14** were less active (Table 4, entries 9 and 10). This behaviour was unexpected since these ligands are less sterically demanding. The catalysts that contain ligands **12a**,**b** and **13a**,**b**, which have OTBDPS groups in positions 2 and 5, have slightly higher activity than those containing ligands **14a**,**b** (Table 4, entries 1, 2 and 5, 6 vs. 9, 10). Unexpectedly, the catalytic systems Rh/**12′a**,**b** were the most actives, while the catalytic systems Rh/**13′a,b**, were found to be the less actives (Table 4, entries 3, 4 and 7, 8).

In all cases, the regioselectivity in the branched aldehyde was higher than 90%, and in some cases it was even higher than 95%. These values are in agreement with those obtained with other rhodium-diphosphite system ligands containing biphenyl moieties.[10,11,28,32]

In general, the enantiomeric excesses obtained with ligands **12–14** in the rhodium-catalysed hydroformylation of styrene were moderate (up to 46%). However, ligands **12a** and **13b** showed higher enantioselectivities than other previously reported with diphosphite ligands derived from 1,2-diols.[22,30] This can be related to the fact that they exclusively coordinate in equatorial-equatorial fashion in the hydridorhodiumdicarbonyl complexes. We have also observed that the value and the sense of the enantiomeric excess were strongly affected by the configuration and substituents of the ligand backbone.

A comparison of the results obtained with ligands **12a–b** with **12c** (Table 3, entries 1, 6 and 13) showed that these systems have similar activities and regioselectivities. However, no enantioselectivity was observed when ligand **12c** was used. This indicates that bulky substituents are needed in *ortho*-positions of the biphenyl moieties if asymmetric induction is to be obtained. This behaviour was also observed in other systems containing diphosphite ligands with the same biphenyl moieties.[10,11,28,32] In ligands containing methoxy groups in the *para*-positions of the biphenyl moieties (ligands **13b–14b**) an increase in the enantioselectivity and a decrease the activity were observed in comparison with the corresponding ligands with *tert*-butyl groups in the *para*-positions of the biphenyl moieties (e.g., Table 4, entries 5 *vs.* 6). Similar behaviour has also been observed in other carbohydrate derivative diphosphite ligands.[10,11,28,32] The behaviour of ligand **12b** was an exception, since when it was used, the activity revealed to be higher and the enantioselectivity lower than ligand **12a**.

The enantioselectivities were higher when bulky substituents were presents in positions 2 and 5 of the tetrahydrofuran ring. This is the case of ligands **12a**, **b** and **13a**, **b** (where X = OTBDPS) which reached enantiomeric excesses up to 43% (Table 4, entries 1, 2 and 5, 6, respectively, see also Figure 15). Unexpectedly, the enantioselectivities were the lowest when a methyl group was in positions 2 and 5 of the tetrahydrofuran ring, **12′a**, **b** and **13′a**, **b** (Table 4, entries 3, 4

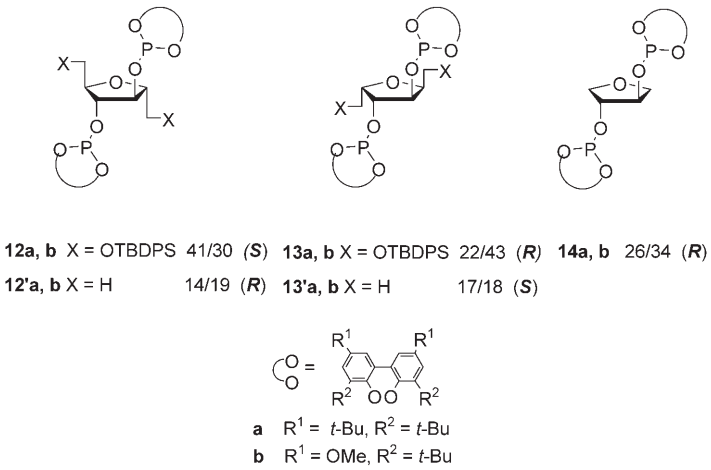

Figure 15. Enantioselectivity values and configuration of the major enantiomer obtained in the hydroformylation of styrene using Rh/**12**–**14** catalytic systems.

and 7, 8, respectively). It could be expected that ligands **14**, which have no substituents in positions 2 and 5 of the tetrahydrofuran ring, provide the lowest enantiomeric excess because they are the more flexible ligands. Nevertheless the enantiomeric excesses were in between the enantioselectivities obtained with ligands **12**–**13** and **12′**–**13′** (Table 4, entries 9 and 10).

It must be noted that the configuration of the major enantiomer produced during the catalysis is governed by both the nature of the substituents and the configuration of the remote stereocentres in positions 2 and 5 of the tetrahydrofuran ring (Table 4, Figure 15). Thus, comparing the hydroformylation results obtained by using ligands **12** and **13** (X = OTBDPS) (Table 4, entries 1 and 2 *vs.* 5 and 6) it can be observed that the enantiomeric excesses were very close but with opposite senses. Similar behaviour was observed for ligands **12′** and **13′** (X = H) (Table 4, entries 3 and 4 *vs.* 7 and 8). However, ligands with the same configuration in positions 2 and 5 of the tetrahydrofuran ring, this is ligands **12**–**12′** and **13**–**13′**, showed an opposite enantiomeric induction (e.g., Table 4, entries 5 and 6 *vs.* 7 and 8). The effect of the remote stereocentres on the enantioselectivity has previously been observed in the asymmetric hydrogenation reaction of enamido esters using diphosphinite ligands **8**–**10** (Figure 2), which have a similar backbone.[18] It can be suggested that the influence of the remote stereocentres on the chiral induction can be due to the interaction of chains at positions 2 and 5 with the biphenyl moieties of the phosphites, which are ultimately responsible for the chirality transfer. It is known that the sterically hindered biphenyl moieties of chiral diphosphites preferentially adopt one configuration, that can change by the interaction with chains in positions 2 and 5.[25,28]

Table 5. Rhodium-catalysed hydroformylation of different vinylarenes using diphosphite **12a**.[a]

Entry	Substrate	% conversion[b]	% regioselectivity[c]	% *ee*
1	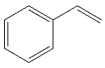	57	96	41 (*S*)
2	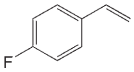	60	97	49 (*S*)
3	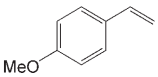	34	96	60 (*S*)
4	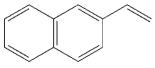	96	94	18 (*S*)

[a] Substrate/Rh = 200, Rh/L = 0.5, substrate 2.7 mmol, [Rh(acac)(CO)$_2$] 0.0135 mmol, P = 20 bar, P(CO/H$_2$) = 1, 15 mL toluene, T = 40 °C, reaction time = 15 h.
[b] % conversion of substrate determined by GC.
[c] % branched aldehyde.

Finally, the diphosphite ligand **12a** was used in the rhodium-catalysed hydroformylation of various substituted vinylarenes. The results are summarised in Table 5. The presence of a fluoro substituent in the *para*-position of the substrate (Table 5, entry 2) did not affect the activity or the regioselectivity. If we compare these results with those obtained in the hydroformylation of styrene (Table 5, entry 1), a slight increase in the enantioselectivity [41 % *ee* (*S*) to 49 % *ee* (*S*)] is observed. When a methoxy group is introduced in the *para*-position the enantioselectivity is enhanced to 60 % *ee* (*S*) (Table 5, entry 3), but the activity is lower. Unexpectedly, the hydroformylation of 2-vinylnaphthalene with diphosphite **12a** evolved with high activity but very low enantioselectivity, 18 % *ee* (*S*) (Table 5, entry 4). In all cases, the sense of the asymmetric induction was the same as that the observed in the styrene hydroformylation. We can conclude that the introduction of substituents in the *para*-position of the substrate affects both the conversion and the enantioselectivity. The fact that the best results were obtained in the rhodium-catalysed hydroformylation of *p*-methoxystyrene agrees with previous report in the literature.[26]

Rhodium-Catalysed Hydrogenation of Methyl Acetamidoacrylate

We have shown that the related diphosphinite ligands **9**–**11** with the same furanoside backbone (Figure 2)[18] showed very high activities in the asymmetric hydrogenation of methyl acetamidoacrylate (total conversion in 5 min at 1 bar of hydrogen pressure and room temperature). Moreover, diphosphite ligands derived from carbohydrates showed very high enantioselectiv-

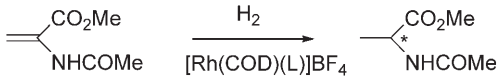

Scheme 6. Hydrogenation of methyl acetamidoacrylate with $[Rh(COD)(L)]BF_4$ catalytic system.

Table 6. Hydrogenation of methyl acetamidoacrylate using $[Rh(L)(COD)]BF_4$ complexes **23**–**25**.[a]

Entry	Ligand	Conversion [%][b]	% *ee*[b]
1	**12a**	7	0
2	**12a**[c]	61	10 (*R*)
3	**12a**[d]	41	45 (*R*)
4	**12b**	6	8 (*R*)
5	**12c**	>99	57 (*R*)
6	**12′a**	21	16 (*R*)
7	**12′a**[c]	59	19 (*R*)
8	**12′b**	74	34 (*R*)
9	**13a**	81	0
10	**13′a**	20	6 (*S*)
11	**14a**	26	13 (*R*)
12	**14b**	17	6 (*R*)

[a] Conditions: 2.5 mL CH_2Cl_2, Rh: 2.5×10^{-6} mol, Rh/substrate = 1/100, room temperature, $P(H_2) = 10$ bar.
[b] % conversion of substrate and enantiomeric excess determined by GC.
[c] Conditions: 5 mL CH_2Cl_2, Rh = 5×10^{-6} mol, Rh/substrate = 1/100, room temperature, $P(H_2) = 50$ bar.
[d] Solvent = CH_2Cl_2/CH_3OH (1/1).

ities in asymmetric hydrogenation.[9] In order to probe the activity of the complexes $[Rh(COD)(L)]BF_4$ (**23**–**25**) in the asymmetric hydrogenation reaction, they were used as catalyst precursors in the hydrogenation of methyl acetamidoacrylate (Scheme 6). The results are summarised in Table 6.

Activities were low for all the complexes tested, and a reaction time of at least 15 h was required to attain full conversion in the best cases. The most active catalytic system was the one with ligand **12c** (Table 6, entry 5). The enantioselectivities were also poor and the major enantiomer, when the enantiomeric excesses were substantial, was always *R*. The results were also best with the catalytic system $[Rh(COD)(\mathbf{12c})]BF_4$ (**23c**). Ligand **12c** has no substituents in the biphenyl moieties, and this may explain the higher activity of the catalytic system containing this ligand. The enantiomeric excesses obtained show that substitution in the biphenyl moieties has a negative effect on the enantioselectivity. Similar behaviour has previously been observed for related xylose derivatives ligands with bulky diphosphites.[11]

In all cases we obtained better results, in activity and enantioselectivity, when dichloromethane was used as a solvent. Complex $[Rh(COD)(\mathbf{12a})]BF_4$ was an exception since the activity and the enantioselectivity increased significantly when the reaction was carried out in dichloromethane/methanol mixture (Table 6, entries 1 *vs.* 3). On the other hand, an increase in hydrogen pressure enhanced the conversion but had a little effect on the enantioselectivity (Table 6, entries 1 and 7 *vs.* 2 and 8, respectively).

The previously described diphosphinite ligands, with the same furanoside backbone (Figure 2),[18] showed very high activities in the asymmetric hydrogenation of methyl acetamidoacrylate using mild conditions, whereas the related diphosphite ligands **12**–**14** showed lower activities in more drastic conditions (10 bar of pressure and room temperature).

This may be due to the greater steric hindrance of the diphosphite ligands (ligand **12c**, without substituents in the biphenyl moieties, showed higher activities than the rest of the related diphosphites) and also to the fact that the diphosphite ligands are less basic than the diphosphinite ligands, since greater basicity favours the oxidative addition of hydrogen which is the rate- and enantioselectivity-determining step of this reaction. On the other hand, in all cases the enantioselectivity of the Rh/diphosphite systems was much lower than with the corresponding Rh/diphosphinite system.

Conclusions

New diphosphite ligands (**12**–**14**) with C_2-symmetry and a tetrahydrofuran backbone were synthesised in moderate to good yields starting from D-glucosamine, D-glucitol and (2*S*,3*S*)-diethyl tartrate. Rhodium cationic complexes containing diphosphite ligands of general formula $[Rh(COD)(L)]BF_4$, (L = **12a**–**c**, **12′a**,**b**, **13a**, **13′a** and **14a**–**b**) were prepared by reacting $[Rh(COD)_2]BF_4$ with the respective ligands. The structures of **12a**, **23a** and **24′a** were proved unambiguously by single crystal X-ray diffraction.

The intermediate species in hydroformylation with diphosphite ligands **12a**, **12b**, **12′a**, **13a**, **13′a** and **14a** were studied by high pressure NMR spectroscopy. The small $^2J_{P\text{-}H}$ coupling constants (2.0 to 9.0 Hz) and the large $^1J_{Rh\text{-}P}$ coupling constants (230.0 to 234.1 Hz) indicate that the ligands coordinate in an equatorial-equatorial fashion in the trigonal-bypiramidal hydridorhodiumcarbonyl species. The low temperature study of the hydridorhodiumcarbonyl species under hydroformylation conditions detected that the phosphorus atoms were non-equivalent, indicating the C_1-symmetry of these complexes.

This new series of diphosphite ligands has been applied to the rhodium-catalysed asymmetric hydroformylation of styrene and related substituted vinylarenes. High regioselectivities to the branched aldehyde (up to 99%) and moderate enantioselectivities (up to 46% *ee*) were obtained in styrene hydroformylation.

In the rhodium-catalysed *p*-methoxystyrene hydroformylation the system containing ligand **12a** reached 60% *ee* which is one of the higher enantioselectivity reported using diphosphites derived from 1,2-diols. We can conclude that the use of strained and hindered backbones can increase the enantioselectivities of rhodium systems containing diphosphites derived from 1,2-diols in comparison to previously reported data. The configuration and substitution of the remote stereocentres in positions 2 and 5 of the tetrahydrofuran ring were observed to have a considerable influence on the enantioselectivity. The most significant result is that changing the configuration of these stereocentres can control the configuration of the major isomer obtained in the hydroformylation reaction.

Rhodium complexes bearing diphosphite ligands were tested in the asymmetric hydrogenation of methyl acetamidoacrylate. The conversions and the enantioselectivities were much lower than those obtained with the corresponding phosphinites, and were mainly influenced by the substitution in the biphenyl moiety and by the configuration of the remote centres in positions 2 and 5 of the tetrahydrofuran ring.

Experimental Section

General Methods

All syntheses were performed using standard Schlenk techniques under argon atmosphere. Solvents were purified by standard procedures. Compounds **15–17**, **19–21** and **22**[18] and phosphorochloridites **18**[21,22] were prepared by methods described previously. All other reagents were used as received. Elemental analyses were performed on a Carlo Erba EA-1108 instrument. ^{1}H, $^{13}C\{^{1}H\}$ and $^{31}P\{^{1}H\}$ NMR spectra were recorded on a Varian Gemini 400 MHz spectrometer. Chemical shifts are relative to $SiMe_4$ (^{1}H and ^{13}C) as internal standard or H_3PO_4 (^{31}P) as external standard. All NMR spectral assignments were determined by COSY and HSQC spectra. Hydroformylation reactions were carried out in a Berghof 100-mL. stainless steel autoclave. Gas chromatographic analyses were run on a Hewlett–Packard HP 5890 A instrument (split/splitless injector, J&W Scientific, HP-5, 25 m column, internal diameter 0.25 mm, film thickness 0.33 mm, carrier gas: 150 kPa He, F.I.D. detector) equipped with a Hewlett–Packard HP3396 series II integrator. Enantiomeric excesses of hydroformylation reactions were measured after oxidation of the aldehydes to the corresponding carboxylic acids on a Hewlett–Packard HP 5890A gas chromatograph (split/splitless injector, J&W Scientific, FS-Cyclodex β-I/P 50 m column, internal diameter 0.2 mm, film thickness 0.33 mm, carrier gas: 100 kPa He, F.I.D. detector). The absolute configuration was determined by comparing of retention times with optically pure (*S*)-(+)-2-phenylpropionic and (*R*)-(−)-2-phenylpropionic acids. Hydrogenation reactions were carried out in a Parr 450-mL multiple reaction vessel autoclave. Conversion and enantiomeric excesses of the reaction crude were measured on a Hewlett–Packard HP 5890A gas chromatograph (split/splitless injector, J&W Scientific, Permabond L-Chirasil-Val, 25 m. column, internal diameter 0.25 mm., carrier gas: 100 kPa He, F.I.D. detector). Single crystal X-ray diffraction structure determinations were carried out using a Bruker-Nonius diffractometer equipped with a APPEX 2 4 K CCD area detector, a FR591 rotating anode with $Mo_{K\alpha}$ radiation, Montel mirrors as monochromator and a Kryoflex low temperature device ($T=$ 100 K), fullsphere data collection omega and phi scans. Programs used: Data collection Apex2 V. 1.0–22 (Bruker-Nonius 2004), data reduction Saint+ Version 6.22 (Bruker-Nonius 2001) and absorption correction SADABS V. 2.10 (2003). Crystal structure solution was achieved using direct methods as implemented in SHELXTL Version 6.10 [G. M. Sheldrick, Universtität Göttingen (Germany), 2000] and visualised using XP program. Missing atoms were subsequently located from difference Fourier synthesis and added to the atom list. Least-squares refinement on F2 using all measured intensities was carried out using the program SHELXTL Version 6.10 [G. M. Sheldrick, Universtität Göttingen (Germany), 2000]. All non-hydrogen atoms were refined including anisotropic displacement parameters.

Synthesis of the Ligands; General Procedure for Synthesising Diphosphites from the Corresponding Diols

To a solution of the diol (0.5 mmol)[18] which had previously been azeotropically dried with toluene (3 × 1 mL), in dry and degassed toluene (5 mL) was added dry pyridine (2.0 mmol). After cooling to 0 °C, the mixture was slowly added to a solution of phosphorochlorohydrite (2.2 mmol), synthesised *in situ* by standard procedure,[21,22] in dry and degassed toluene (6 mL) and dry pyridine (2.2 mmol). The mixture was allowed to warm to room temperature and stirred overnight. The mixture was then filtered to eliminate the pyridine salts, and the filtrate was concentrated to dryness. The white foam obtained was purified by chromatographic techniques.

3,4-Bis-*O*-[(3,3′,5,5′-tetra-*tert*-butyl-1,1′-biphenyl-2,2′-diyl)-phosphite]-1,6-di-*O*-(*tert*-butyldiphenylsilyl)-2,5-anhydro-D-mannitol (12a): The synthesis of **12a** was carried out in accordance with the general procedure from 0.3 g (0.47 mmol) of diol **17** in 5 mL of dry and degassed toluene and 0.2 mL (2.4 mmol) of dry pyridine, and 2.1 mmol of phosphorochlorohydrite **18a** in 6 mL of toluene and 0.2 mL (2.4 mmol) of pyridine. The reaction mixture was purified by flash column chromatography (eluent: toluene $R_f=0.9$) to afford **12a** as a white solid; yield: 0.22 g (31%)

Single crystal X-ray diffraction: Crystals of **12a** were obtained by slow diffusion of hexane into a solution of **12a** in dichloromethane. Empirical formula: $C_{106}H_{154}O_{9.5}P_2Si_2$, formula weight: 679.36, temperature: 100(2) K, wavelength: 0.71073 Å, crystal system: monoclinic, space group: $P2_1$, unit cell dimensions: $a=14.6938(11)$ Å, $b=24.842(2)$ Å, $c=15.0146(12)$ Å, $\beta=109.112(2)°$, $V=5178.6(7)$ Å^3, $Z=2$, density (calculated): 1.089 Mg/m^3, μ (Mo-K$_\alpha$): 0.118 mm^{-1}, crystal size: $0.40\times0.40\times0.40$ mm^3, theta range for data collection: 2.81 to 36.88°, reflections collected: 86383, independent reflections: 46995 [R(int) = 0.0401], absorption correction: SADABS (Bruker-Nonius), refinement method: full-matrix least-squares on F^2, data/restraints/parameters:

46995/1/1125, goodness-of-fit on F^2: 1.018, final R indices [I > 2 sigma(I)]: $R1 = 0.0719$, $wR2 = 0.2001$, R indices (all data): $R1 = 0.0933$, $wR2 = 0.2190$, absolute structure parameter: 0.16(5), largest diff. peak and hole: 1.050 and -0.584 e Å^{-3}. The ligand crystallises as a solvate with two molecules of *n*-hexane and two disordered positions of water (in total $^1/_2$ molecule of water without hydrogen atoms) in the elementary cell. The measured compound crystallises as a racemic twin (74:16).

3,4-Bis-*O*-[(3,3′-di-*tert*-butyl-5,5′-dimethoxy-1,1′-biphenyl-2,2′-diyl)phosphite]-1,6-di-*O*-(*tert*-butyldiphenylsilyl)-2,5-anhydro-D-mannitol (12b): Following the general procedure 0.3 g (0.47 mmol) of diol **17** in 5 mL of dry and degassed toluene and 0.2 mL (2.4 mmol) of dry pyridine were treated with 2.1 mmol of the phosphorochlorohydrite **18b** dissolved in 6 mL of toluene and 0.2 mL (2.4 mmol) of pyridine. After the work-up the reaction mixture was purified by flash column chromatography (eluent: toluene $R_f = 0.75$) to afford **12b** as a white solid; yield: 0.28 g (42%).

3,4-Bis-*O*-[(1,1′-biphenyl-2,2′-diyl)phosphite]-1,6-di-*O*-(*tert*-butyl-diphenylsilyl)-2,5-anhydro-D-mannitol (12c): Following the general procedure 0.25 g (0.40 mmol) of diol **17** in 2.5 mL of dry and degassed toluene and 0.1 mL (1.6 mmol) of dry pyridine were treated with 1.6 mmol of phosphorochlorohydrite **18c** dissolved in 4 mL of toluene and 0.1 mL (1.6 mmol) of pyridine. After the work-up the remaining residue was purified by flash column chromatography (eluent: hexane/ethyl acetate 100:2 $R_f = 0.6$) to afford **12c** as a white solid; yield: 0.21 g (50%).

3,4-Bis-*O*-[(3,3′,5,5′-tetra-*tert*-butyl-1,1′-biphenyl-2,2′-diyl)-phosphite]-1,6-dideoxy-2,5-anhydro-D-mannitol (12′a): The synthesis of **12′a** was carried out in accordance with the general procedure from 0.15 g (1.14 mmol) of diol **17**' in 10 mL of dry and degassed toluene and 0.5 mL (5.7 mmol) of dry pyridine and 4.6 mmol of phosphorochlorohydrite **18a** dissolved in 12 mL of toluene and 0.5 mL (5.7 mmol) of pyridine. After the work-up the obtained residue was purified by flash column chromatography (eluent: toluene $R_f = 0.9$) to afford**12′a** as a white solid; yield: 0.84 g (72%).

3,4-Bis-*O*-[(3,3′-di-*tert*-butyl-,5,5′-dimethoxy-1,1′-biphenyl-2,2′-diyl)phosphite]-1,6-dideoxy-2,5-anhydro-D-mannitol (12′b): Following the general procedure 0.15 g (1.14 mmol) of diol **17′** in 10 mL of dry and degassed toluene and 0.5 mL (5.7 mmol) of dry pyridine were treated with 4.6 mmol of phosphorochlorohydrite **18b** dissolved in 12 mL of toluene and 0.5 mL (5.7 mmol) of pyridine. After the work-up the obtained residue was purified by flash column chromatography (eluent: toluene $R_f = 0.9$) to afford **12′b** as a white solid; yield: 0.4 g (42%).

3,4-Bis-*O*-[(3,3′,5,5′-tetra-*tert*-butyl-1,1′-biphenyl-2,2′-diyl)-phosphite]-1,6-di-*O*-(*tert*-butyldiphenylsilyl)-2,5-anhydro-L-iditol (13a): Following the general procedure 0.25 g (0.40 mmol) of diol **21** in 2.5 mL of dry and degassed toluene and 0.1 mL (1.6 mmol) of dry pyridine were treated with 1.6 mmol of phosphorochlorohydrite **18a** dissolved in 4 mL of toluene and 0.1 mL (1.6 mmol) of pyridine. After the work-up the obtained residue was purified by flash column chromatography (eluent: toluene $R_f = 0.9$) to afford **13a** as a white solid; yield: 0.25 g (42%).

3,4-Bis-*O*-[(3,3′-di-*tert*-butyl-5,5′-dimethoxy-1,1′-biphenyl-2,2′-diyl)phosphite]-1,6-di-*O*-(*tert*-butyldiphenylsilyl)-2,5-anhydro-L-iditol (13b): Following the general procedure 0.25 g (0.40 mmol) of diol **21** in 4 mL of dry and degassed toluene and 0.1 mL (1.6 mmol) of dry pyridine were treated with 1.6 mmol of phosphorochlorohydrite **18b** dissolved in 4 mL of toluene and 0.1 mL (1.6 mmol) of pyridine. After the work-up the obtained residue was purified by flash column chromatography (eluent: toluene $R_f = 0.6$) to afford **13b** as a white solid; yield: 0.18 g (32%).

3,4-Bis-*O*-[(3,3′,5,5′-tetra-*tert*-butyl-1,1′-biphenyl-2,2′-diyl)-phosphite]-1,6-dideoxy-2,5-anhydro-L-iditol (13′a): The synthesis of **13′a** was carried out in accordance with the general procedure from 0.075 g (0.57 mmol) of diol **21′** in 5 mL of dry and degassed toluene and 0.25 mL (2.9 mmol) of dry pyridine, and 2.3 mmol of phosphorochlorohydrite **18a** dissolved in 6 mL of toluene and 0.25 mL (2.9 mmol) of pyridine. The mixture was stirred overnight, the salts were filtered and the white foam was purified by flash column chromatography (eluent: toluene $R_f = 0.9$) to afford **13′a** as a white solid; yield: 0.53 g (92%).

3,4-Bis-*O*-[(3,3′-di-*tert*-butyl-,5,5′-dimethoxy-1,1′-biphenyl-2,2′-diyl)phosphite]-1,6-dideoxy-2,5-anhydro-L-iditol (13′b): The synthesis of **13′b** was carried out in accordance with the general procedure from 0.075 g (0.57 mmol) of diol **21′** in 5 mL of dry and degassed toluene and 0.25 mL (2.9 mmol) of dry pyridine, and 2.3 mmol of phosphorochlorohydrite **18b** dissolved in 6 mL of toluene and 0.25 mL (2.9 mmol) of pyridine. After the work-up the obtained residue was purified by flash column chromatography (eluent: toluene $R_f =$ 0.5) to afford **13′b** as a white solid; yield: 0.53 g (64%).

(3*R*,4*R*)-(−)-3,4-Bis-*O*-[(3,3′,5,5′-tetra-*tert*-butyl-1,1′-biphenyl-2,2′-diyl)phosphite]-tetrahydrofuran (14a): Following the general procedure from 0.15 g (1.44 mmol) of diol **22** in 14 mL of dry and degassed toluene and 0.7 mL (5.7 mmol) of dry pyridine, were treated with 7 mmol of phosphorochlorohydrite **18a** dissolved in 15 mL of toluene and 0.7 mL (5.7 mmol) of pyridine. After the work-up the obtained residue was purified by flash column chromatography (eluent: toluene $R_f = 0.9$) to afford **14a** as a white solid; yield: 1.00 g (75%).

3,4-Bis-*O*-[(3,3′-di-*tert*-butyl-5,5′-dimethoxy-1,1′-biphenyl-2,2′-diyl)phosphite]-tetrahydrofuran (14b): Following the general procedure 0.15 g (1.14 mmol) of diol **22** in 10 mL of dry and degassed toluene and 0.5 mL (5.7 mmol) of dry pyridine, were treated with 4.6 mmol of phosphorochlorohydrite **18b** dissolved in 12 mL of toluene and 0.5 mL (5.7 mmol) of pyridine. After the work-up the obtained residue was purified by flash column chromatography (eluent: toluene $R_f =$ 0.9) to afford **14b** as a white solid; yield: 0.3 g (29%).

Synthesis of Rhodium Complexes; General Procedure for Synthesizing [Rh(COD)(L)]BF_4, L = Diphosphite

The complexes were prepared by adding 1.1 equivalents of diphosphinite ligand to a solution of $[Rh(COD)_2]BF_4$ in the minimum volume of CH_2Cl_2. The mixture was then stirred for 30 min, and the solvent was removed under vacuum. The residue was washed with dry hexane first and then with dry ether in order to remove the excess diphosphite and free cyclooctadiene. Characterisation details of rhodium complexes [Rh(COD)(L)]BF_4, **23--25**, where L = diphosphite ligands **12--14** are collected in the Supporting Information.

[Rh(COD)(12a)]BF_4 (23a): Beginning with 0.015 g (0.036 mmol) of $[Rh(COD)_2]BF_4$ in the minimum quantity

of CH_2Cl_2, 0.060 g (0.040 mmol) of diphosphite **12a** and following the general procedure, 0.054 g (83%) of complex [Rh(COD)(**12a**)]BF_4 **23a** was obtained as a yellow solid.

Single crystal X-ray diffraction. Crystals of [Rh(COD)(**12a**)]BF_4 (**23a**) were obtained by slow diffusion of hexane into a solution of [Rh(COD)(**12a**)]BF_4 (**23a**) in dichloromethane. Empirical formula: $C_{103}H_{140}BCl_2F_4O_{9.50}P_2RhSi_2$, formula weight: 1908.89, temperature: 100(2) K, wavelength: 0.71073 Å, crystal system: orthorhombic, space group: $P2_12_12_1$, unit cell dimensions: $a=19.512(3)$ Å, $b=20.172(3)$ Å, $c=26.249(4)$ Å, $V=10332(3)$ Å^3, $Z=4$, density (calculated): 1.227 Mg/m^3, μ (Mo K_α): 0.332 mm^{-1}, crystal size: $0.20\times0.10\times0.04$ mm^3, theta range for data collection: 2.74 to 30.18°, reflections collected: 125396, independent reflections: 30370 [R(int)=0.0744], absorption correction: SADABS (Bruker-Nonius), refinement method: full-matrix least-squares on F^2, data/restraints/parameters: 30370/14/1393, goodness-of-fit on F^2: 1.013, final R indices [I>2 sigma(I)]:$R1=0.0492$, $wR2=0.1139$, R indices (all data): $R1=0.0798$, $wR2=0.1282$, absolute structure parameter: −0.022(15), largest diff. peak and hole: 1.186 and −0.973 e Å^{-3}.Compound [Rh(COD)(**12a**)]BF_4 (**23a**) crystallizes as a cation together with a BF_4 anion, a disordered water molecule (occupancy of 0.5 and without hydrogen atoms) and two disordered positions of dichloromethane. The measured compound crystallises in a pure chiral structure.

[Rh(COD)(12b)]BF_4 (23b): Beginning with 0.012 g (0.030 mmol) of [Rh(COD)$_2$]BF_4 in the minimum quantity of CH_2Cl_2 and 0.046 g (0.032 mmol) of diphosphite **12b** and following the general procedure, 0.030 g (61%) of complex [Rh(COD)(**12b**)]BF_4 **23b** was obtained as a yellow solid.

[Rh(COD)(12c)]BF_4 (23c): Beginning with 0.025 g (0.061 mmol) of [Rh(COD)$_2$]BF_4 in 10 mL of CH_2Cl_2 and 0.074 g (0.067 mmol) of diphosphite **12c** and following the general procedure, 0.054 g (65%) of complex [Rh(COD)(**12c**)]BF_4 **23c** was obtained as a pale yellow solid.

[Rh(COD)(12′a)]BF_4 (23′a): Beginning with 0.025 g (0.062 mmol) of [Rh(COD)$_2$]BF_4 in the minimum quantity of CH_2Cl_2, 0.069 g (0.068 mmol) of diphosphite **12′a** and following the general procedure, 0.068 g (81%) of complex [Rh(COD)(**12′a**)]BF_4 **23′a** was obtained as a yellow solid.

[Rh(COD)(12′b)]BF_4 (23′b): Beginning with 0.021 g (0.052 mmol) of [Rh(COD)$_2$]BF_4 in the minimum quantity of CH_2Cl_2, 0.050 g (0.055 mmol) of diphosphite **12′b** and following the general procedure, 0.047 g (76%) of complex [Rh(COD)(**12′b**)]BF_4 **23′b** was obtained as a yellow-orange solid.

[Rh(COD)(13a)]BF_4 (24a): Beginning with 0.015 g (0.036 mmol) of [Rh(COD)$_2$]BF_4 in the minimum quantity of CH_2Cl_2, 0.062 g (0.041 mmol) of diphosphite **13a** and following the general procedure, 0.054 g (83%) of complex [Rh(COD)(**13a**)]BF_4 **24a** was obtained as a yellow solid.

[Rh(COD)(13′a)]BF_4 (24′a): Beginning with 0.025 g (0.062 mmol) of [Rh(COD)$_2$]BF_4 in the minimum quantity of CH_2Cl_2, 0.069 g (0.068 mmol) of diphosphite **13′a** and following the general procedure, 0.068 g (81%) of complex [Rh(COD)(**13′a**)]BF_4 **24′a** was obtained as a yellow solid.

Single crystal X-ray diffraction. Crystals of [Rh(COD)(**13′a**)]BF_4 (**24′a**) were obtained by slow diffusion of hexane into a solution of [Rh(COD)(**13′a**)]BF_4 (**24′a**) in dichloromethane. Empirical formula: $C_{143}H_{210}B_2Cl_6F_8O_{14}P_4Rh_2$, formula weight: 2869.13, temperature: 100(2) K, wavelength: 0.71073 Å, crystal system: orthorhombic, space group: $P2_12_12_1$, unit cell dimensions: $a=19.1067(15)$ Å, $b=26.855(2)$ Å, $c=30.828(3)$ Å, $V=15818(2)$ Å^3, $Z=4$, density (calculated):1.205 Mg/m^3, μ (Mo K_α): 0.413 mm^{-1}, crystal size: $0.20\times0.04\times0.02$ mm^3, theta range for data collection: 2.50 to 30.73°, reflections collected: 209015, independent reflections: 48854 [R(int)=0.0598], absorption correction: SADABS (Bruker-Nonius), refinement method: full-matrix least-squares on F^2, data/restraints/parameters: 48854/0/1719, goodness-of-fit on F^2: 1.068, final R indices [I>2 sigma(I)]: $R1=0.0661$, $wR2=0.1780$, R indices (all data): $R1=0.0867$, $wR2=0.1923$, absolute structure parameter: 0.000(18), largest diff. peak and hole: 1.748 and −1.039 e Å^{-3}. Compound [Rh(COD)(**13′a**)]BF_4 (**24′a**) crystallises with two independent cations in the elementary cell. The crystal cell also contains two BF_4 anions and four disordered positions of dichloromethane molecules with a total occupancy of 3. The independently obtained cationic structures have different conformations. The measured compound crystallises in a pure chiral structure.

[Rh(COD)(14a)]BF_4 (25a): Beginning with 0.025 g (0.062 mmol) of [Rh(COD)$_2$]BF_4 in the minimum quantity of CH_2Cl_2, 0.068 g (0.068 mmol) of diphosphite **14a** and following the general procedure, 0.059 g (75%) of complex [Rh(COD)(**14a**)]BF_4 **25a** was obtained as a yellow-orange solid.

[Rh(COD)(14b)]BF_4 (25a): Beginning with 0.025 g (0.062 mmol) of [Rh(COD)$_2$]BF_4 in the minimum quantity of CH_2Cl_2, 0.061 g (0.068 mmol) of diphosphite **14b** and following the general procedure, 0.054 g (79%) of complex [Rh(COD)(**14b**)]BF_4 **25a** was obtained as a yellow-orange solid.

In Situ High-Pressure NMR Experiments; General Procedure

In a typical experiment, a sapphire tube (ø10 mm) was filled under argon with a solution of [Rh(acac)(CO)$_2$] (2.10^{-2} M) and ligand (molar ratio PP/Rh=1.1) in toluene-d_8 (2 mL). The solution was analysed and then the HP NMR tube was purged three times with CO and pressurised to the appropriate pressure of CO/H_2. After a reaction time of 15 h during which the solution was shaken at 80 °C of temperature, the solution was analysed. Characterisation details of [Rh(acac)(L)] and [RhH(CO)$_2$(L)] (L: **12a–14a**, **12b**) species are collected in the Supporting Information.

Hydroformylation Experiments

In a typical experiment, the autoclave was purged three times with CO. The solution was formed from [Rh(acac)(CO)$_2$] (0.013 mmol), diphosphite (0.015 mmol) and styrene (13 mmol) in toluene (15 mL). The autoclave was pressurised to the desired pressure. After the desired reaction time, the autoclave was cooled to room temperature and depressurised. The reaction mixture was analysed by gas chromatography. The aldehydes obtained from the hydroformylation were oxidised to carboxylic acids to determine the enantiomeric excess.

Hydrogenation Experiments

The experiments were prepared in a multiple reaction vessel autoclave in a glovebox. After the addition of the substrate to a solution of $[Rh(COD)(L)]BF_4$ (2.5×10^{-3} mmol) in the corresponding solvent (2.5 mL) the autoclave was pressurised to the desired pressure with hydrogen. After the desired reaction time the autoclave was depressurised. The reaction mixture was analysed by gas chromatography.

Supporting Information

Experimental details for the characterization of all new compounds and the hydrofomylation and hydrogenation reaction procedures are collected in the Supporting Information. Crystallographic data (excluding structure factors) for the structures reported in this paper have been deposited with the Cambridge Crystallographic Data Centre as supplementary publication no. CCDC 610289–610291. Copies of the data can be obtained free of charge on application to CCDC, 12 Union Road, Cambridge CB2 1EZ, UK [fax.: (internat.) + 44 1223/336–033; e-mail: deposit@ccdc.cam.ac.uk].

Acknowledgements

We thank the Spanish Government, Ministerio de Educación y Cultura, (CTQ2004–04412/BQU, CTQ2005–03124 and Consolider Ingenio 2010,CSD2006–0003) and the Generalitat de Catalunya (2005SGR007777 and Distinction for Research Promotion, 2003 C.C.) for their financial support. With the support of the Departament d'Universitats, Recerca i Societat de la Informació i del Fons Social Europeu for a FPI grant (M.R.A.).

References

[1] a) M. Diéguez, O. Pàmies, C. Claver, *Chem. Rev.* **2004**, *104*, 3189–3215; b) M. Diéguez, O. Pàmies, A. Ruiz, Y. Diaz, S. Castillón, C. Claver, *Coord. Chem. Rev.* **2004**, *248*, 2165–2192; c) S. Castillón, C. Claver, Y. Diaz, *Chem. Soc. Rev.* **2005**, *34*, 702–713.

[2] a) R. Selke, H. Pracejus, *J. Mol. Catal.* **1986**, *37*, 213–225; b) T. V. RajanBabu, A. L. Casalnuovo, *J. Am. Chem. Soc.* **1992**, *114*, 6265–6266; c) R. Selke, M. Schwarze, H. Baudisch, I. Grassert, M. Michalik, G. Oehme, N. Stoll, B. Costisella, *J. Mol. Catal.* **1993**, *84*, 223–237; d) T. V. RajanBabu, T. A. Ayers, A. L. Casalnuovo, *J. Am. Chem. Soc.* **1994**, *116*, 4101–4102; e) T. V. RajanBabu, B. Radetich, K. K. You, T. A. Ayers, A. L. Casalnuovo, J. C. Calabrese, *J. Org. Chem.* **1999**, *64*, 3429–3447.

[3] A. L. Casalnuovo, T. V. Rajanbabu, T. A. Ayers, T. H. Warren, *J. Am. Chem. Soc.* **1994**, *116*, 9869–9882.

[4] T. V. RajanBabu, T. A. Ayers, G. A. Halliday, K. K. You, J. C. Calabrese, *J. Org. Chem.* **1997**, *62*, 6012–6025.

[5] M. Diéguez, O. Pàmies, A. Ruiz, S. Castillón, C. Claver, *Chem. Commun.* **2000**, 1607–1608.

[6] a) M. Diéguez, O. Pàmies, A. Ruiz, C. Claver, S. Castillón, *Chem. Eur. J.* **2001**, *7*, 3086–3094; b) M. Diéguez, O. Pàmies, A. Ruiz, C. Claver, *New J. Chem.* **2002**, *26*, 827–833.

[7] a) C. J. Cobley, J. Klosin, C. Qin, G. T. Whiteker, *Org. Lett.* **2004**, *6*, 3277–3280; b) C. J. Cobley, K. Gardner, J. Klosin, C. Praquin, C. Hill, G. T. Whiteker, A. Zanotti-Gerosa, J. L. Petersen, K. A. Abboud, *J. Org. Chem.* **2004**, *69*, 4031–4040.

[8] a) J. E. Babin, G. T. Whiteker, (Union Carbide Chem. Plastics Techn. Co.), *World Patent* WO 93/03839, **1993**; *Chem. Abs.* **1993**, *119*, P159872; b) K. Nozaki, N. Sakai, T. Nanno, T. Higashijima, S. Mano, T. Horiuchi, H. Takaya, *J. Am. Chem. Soc.* **1997**, *119*, 4413–4423.

[9] O. Pamies, M. Dieguez, G. Net, A. Ruiz, C. Claver, *J. Org. Chem.* **2001**, *66*, 8364–8369.

[10] M. Diéguez, A. Ruiz, C. Claver, *J. Org. Chem.* **2002**, *67*, 3796–3801.

[11] O. Pàmies, G. Net, A. Ruiz, C. Claver, *Tetrahedron: Asymmetry* **2000**, *11*, 1097–1108.

[12] S. Jansat, M. Gomez, K. Philippot, G. Muller, E. Guiu, C. Claver, S. Castillon, B. Chaudret, *J. Am. Chem. Soc.* **2004**, *126*, 1592–1593.

[13] M. T. Reetz, T. Neugebauer, *Angew. Chem. Int. Ed.* **1999**, *38*, 179–181.

[14] a) A. Börner, J. Holz, G. Voss, R. Stürmer, German Patent DE 48 084, **1997**; b) J. Holz, M. Quirmbach, U. Schmidt, D. Heller, R. Sturmer, A. Börner, *J. Org. Chem.* **1998**, *63*, 8031–8034; c) J. Holz, D. Heller, R. Sturmer, A. Börner, *Tetrahedron Lett.* **1999**, *40*, 7059–7062; d) W. Li, Z. Zhang, D. Xiao, X. Zhang, *Tetrahedron Lett.* **1999**, *40*, 6701–6704; e) W. Li, Z. Zhang, D. Xiao, X. Zhang, *J. Org. Chem.* **2000**, *65*, 3489–3496; f) T. V. RajanBabu, Y.-Y. Yan, S. Shin, *J. Am. Chem. Soc.* **2001**, *123*, 10207–10213; g) J. Holz, R. Sturmer, U. Schmidt, H. J. Drexler, D. Heller, H. P. Krimmer, A. Börner, *Eur. J. Org. Chem.* **2001**, 4615–4624; h) A. Bayer, P. Murszat, U. Thewalt, B. Rieger, *Eur. J. Inorg. Chem.* **2002**, 2614–2624.

[15] Y. Y. Yan, T. V. RajanBabu, *Org. Lett.* **2000**, *2*, 4137–4140.

[16] a) A. T. Axtell, C. J. Cobley, J. Klosin, G. T. Whiteker, A. Zanotti-Gerosa, K. A. Abboud, *Angew. Chem. Int. Ed.* **2005**, *44*, 5834–5838; b) T. P. Clark, C. R. Landis, S. L. Freed, J. Klosin, K. A. Abboud, *J. Am. Chem. Soc.* **2005**, *127*, 5040–5042.

[17] J. K. Huang, E. Bunel, A. Allgeier, J. Tedrow, T. Storz, J. Preston, T. Correll, D. Manley, T. Soukup, R. Jensen, R. Syed, G. Moniz, R. Larsen, M. Martinelli, P. J. Relder, *Tetrahedron Lett.* **2005**, *46*, 7831–7834.

[18] M. Aghmiz, A. Aghmiz, Y. Diaz, A. Masdeu-Bulto, C. Claver, S. Castillón, *J. Org. Chem.* **2004**, *69*, 7502–7510.

[19] W. R. Jackson, C. G. Lovel, *Aust. J. Chem.* **1982**, *35*, 2069–2075.

[20] R. D. Guthrie, I. D. Jenkins, J. J. Watters, M. W. Wright, R. Yamasaki, *Aust. J. Chem.* **1982**, *35*, 2169–2173.

[21] T. Jongsma, M. Fossen, G. Challa, P. W. N. M. van Leeuwen, *J. Mol. Catal.* **1993**, *83*, 17–35.

[22] G. J. H. Buisman, P. C. J. Kamer, P. W. N. M. van Leeuwen, *Tetrahedron: Asymmetry* **1993**, *4*, 1625–1634.

[23] a) R. J. Rafka, B. J. Morton, *Carbohydr. Res.* **1994**, *260*, 155–158; b) S. Cassel, C. Debaig, T. Benvegnu, P.

Chaimbault, M. Lafosse, D. Plusquellec, P. Rollin, *Eur. J. Org. Chem.* **2001**, 875–896.
[24] A. Terfort, *Synthesis* **1992**, 951–953.
[25] G. J. H. Buisman, L. A. van Der Veen, A. Klootwijk, W. G. J. De Lange, P. C. J. Kamer, P. W. N. M. van Leeuwen, D. Vogt, *Organometallics* **1997**, *16*, 2929–2939.
[26] a) E. Guimet, J. Parada, M. Diéguez, A. Ruiz, C. Claver, *Appl. Catal. A* **2005**, *282*, 215–220; b) P. Uriz, E. Fernandez, N. Ruiz, C. Claver, *Inorg. Chem. Commun.* **2000**, *3*, 515–519; c) M. Diéguez, O. Pàmies, G. Net, A. Ruiz, C. Claver, *Tetrahedron: Asymmetry* **2001**, *12*, 651–656.
[27] G. Franciò, W. Leitner, *Chem. Commun.* **1999**, 1663–1664.
[28] P. W. N. M. van Leeuwen, C. Claver, *Rhodium Catalyzed Hydroformylation,* Vol. 22, Kluwer Academic Press, Dordrecht, **2000**.
[29] G. J. H. Buisman, M. E. Martin, E. J. Vos, A. Klootwijk, P. C. J. Kamer, P. W. N. M. van Leeuwen, *Tetrahedron: Asymmetry* **1995**, *6*, 719–738.
[30] G. J. H. Buisman, E. J. Vos, P. C. J. Kamer, P. W. N. M. van Leeuwen, *J. Chem. Soc., Dalton Trans.* **1995**, 409–417.
[31] G. J. H. Buisman, L. A. van der Veen, P. C. J. Kamer, P. van Leeuwen, *Organometallics* **1997**, *16*, 5681–5687.
[32] M. Diéguez, O. Pàmies, C. Claver, *Tetrahedron: Asymmetry* **2004**, *15*, 2113–2122.

